The ferroelectric phase transition in small spherical particles

1997 J. Phys.: Condens. Matter 9 4955

(http://iopscience.iop.org/0953-8984/9/23/019)

J. Phys.: Condens. Matter **9** (1997) 4955–4965. Printed in the UK PII: S0953-8984(97)77916-5

The ferroelectric phase transition in small spherical particles

I Rychetský and O Hudák

Institute of Physics, Czech Academy of Science, Na Slovance 2, 18040 Prague, Czech Republic

Received 18 September 1996

Abstract. The ferroelectric phase transition in a small particle depends on its size. Analytical results concerning the size dependence of the transition temperature, and the polarization profile in the ferroelectric phase have been obtained within a phenomenological model, which has been previously studied only numerically. The model does not take into consideration the depolarization field, assuming full compensation of surface charges. The dynamic susceptibility deviates from Debye-like behaviour in exhibiting a broadening at higher frequencies. The static susceptibility obeys the Curie–Weiss law, and exhibits a similar divergency at the point of the size-driven transition.

1. Introduction

The size effect is undoubtedly important for small ferroelectric particles as regards the explanation of the ferroelectric phase transition and dielectric properties of powders, composites, and ceramics. The transition temperature is usually lower than the Curie temperature, and has turned out to depend on the particle size. It decreases with decreasing particle diameter in $BaTiO_3$ [1], $PbTiO_3$ [2], and KDP [3], and there is no transition below a critical size.

In some cases the transition temperature can be higher than the Curie temperature. This assertion is supported by the observations for thin films of $KNbO_3$ [4] and TGS [5, 6], in which both an increase and a decrease of the transition temperature were observed, probably depending on the sample preparation.

The dielectric constant decreases with decreasing particle size in $PbTiO_3$ composites [7], and it was proposed that this occurs due to the gradual creation of a multidomain state in the larger particles. An unusual peak of the dielectric constant versus the particle size was observed for $BaTiO_3$ [8].

Two main theoretical explanations of the size effects for composites are proposed.

The first concept stresses the significance of the depolarization field and a space charge layer, which try to break up the particle into domains of different polarization. The multidomain ferroelectric state disappears in small enough particles, and concomitantly the dielectric constant exhibits a peak [9].

Within the second approach, full compensation of the surface charges is assumed to have taken place after some time, and thus the depolarization field does not then exist. Instead, a surface layer with a different transition temperature to that of the bulk is considered. This causes the shift of the phase transition in the particle, and an inhomogeneous distribution of the polarization [10]. In reference [10], the authors studied the static properties by means of numerical calculations.

0953-8984/97/234955+11$19.50

In the present paper we have analytically solved the latter phenomenological model for the second-order phase transition in the spherical particle. The generalization of this model enables us to obtain the temperature- and size-dependent dynamical dielectric susceptibility of the particle.

2. The model

The phase transition in a ferroelectric particle has been successfully described within the Landau theory. For the second-order phase transition, the total free energy reads [10]

$$\mathcal{F} = \int_{(V)} \mathrm{d}^3\boldsymbol{r}\ \left[\frac{1}{2}A(T-T_C)P^2 + \frac{1}{4}BP^4 + \frac{1}{2}D(\boldsymbol{\nabla}P)^2 - EP\right] + \int_{(S)} \mathrm{d}^2\boldsymbol{r}\ \left[\frac{1}{2}D\delta^{-1}P^2\right] \tag{1}$$

where P is the position-dependent polarization, and T_C is the Curie temperature of the bulk crystal. The first term describes the interior region with spatially independent positive interaction constants A, B, D, while the second one is included to account for the surface. The length δ characterizes the surface, and depends also on the surroundings of the particle. Its value can be either positive or negative. One can obtain the polarization profile by minimizing the free energy (1). To simplify the problem, we shall consider a particle of spherical shape, with the radius R. For the sake of simplicity, we further assume that the polarization lies in a single direction, and that its value $P(r)$ depends on the radius r only. The free energy in spherical coordinates becomes [10]

$$\frac{\mathcal{F}}{4\pi} = \int_0^R \mathrm{d}r\ r^2\left[\frac{1}{2}A(T-T_C)P^2 + \frac{1}{4}BP^4 + \frac{1}{2}D(\boldsymbol{\nabla}P)^2 - EP\right] + \frac{1}{2}DR^2\delta^{-1}P_S^2 \tag{2}$$

where $P_S \equiv P(r=R)$. On the basis of geometrical considerations, it was proposed that the coefficient δ depends on the radius R as follows [10]:

$$\frac{1}{\delta} = \frac{5}{2R} + \frac{1}{\delta_\infty}\left(1 - \frac{a_0}{2R}\right) \tag{3}$$

where δ_∞ is the limiting value corresponding to the flat surface ($R=\infty$), and a_0 is the lattice spacing. For the sake of simplicity, we shall further assume a size-independent δ. Nevertheless, the expression (3) could be taken into account at the end, by a simple substitution into the formulae obtained. It was stressed in reference [10] that δ becomes positive for small enough particles in the case of negative δ_∞ as well.

3. Size dependence of the Curie temperature

The Curie temperature can be calculated by analysing the stability of the equilibrium state $P(r)$ against small perturbations $\delta P(r)$. The linearized equations of motion for $\delta P(r,t)$ and for $\delta P_S(t)$ can be derived as follows:

$$\rho\frac{\partial^2\delta P}{\partial t^2} + \Gamma\frac{\partial\delta P}{\partial t} = \frac{1}{r}\frac{\partial^2(r\,\delta P)}{\partial r^2} - \left(\frac{A(T-T_C)}{D} + 3\frac{B}{D}P(r)^2\right)\delta P \tag{4}$$

$$\rho_S\frac{\partial^2\delta P^S}{\partial t^2} + \Gamma_S\frac{\partial\delta P^S}{\partial t} = -\left(\frac{\partial\delta P^S}{\partial r} + \frac{1}{\delta}\delta P^S\right) \tag{5}$$

where ρ and ρ_S are densities, and Γ and Γ_S are friction coefficients (divided by D) for the bulk and the surface. To analyse the stability of the para-phase we put $P(r)\equiv 0$, and consider a single-harmonic perturbation: $\delta P = \delta P_\omega\,\mathrm{e}^{\mathrm{i}\omega t}$ and $\delta P^S = \delta P^S_\omega\,\mathrm{e}^{\mathrm{i}\omega t}$. The frequency

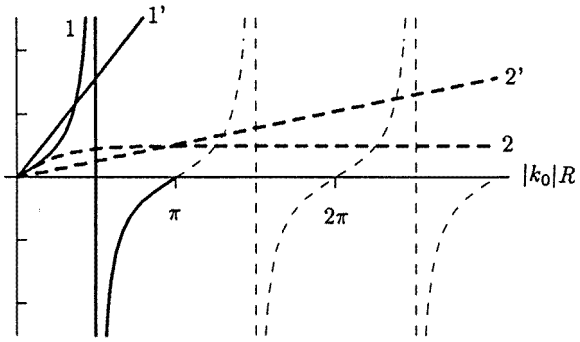

Figure 1. A graphical representation of certain equations: equation (11) ($\delta > 0$, $T_P < T_C$); curves 1: $\tan k_0 R$; and 1′: $k_0 R/(1 - R\delta^{-1})$; and equation (13) ($\delta < 0$, $T_P < T_C$); curves 2: $\tanh |k_0| R$; and 2′: $|k_0| R/(1 - R\delta^{-1})$.

is, in general, a complex number reflecting the damping. The equations for the amplitudes become

$$\frac{\partial^2 (r\,\delta P_\omega)}{\partial r^2} + \left(k_\omega^2 - 3\frac{B}{D} P(r)^2 \right) r\,\delta P_\omega = 0 \tag{6}$$

and

$$\frac{\partial \delta P_\omega^S}{\partial r} + \delta_\omega^{-1}\,\delta P_\omega^S = 0 \tag{7}$$

where

$$k_\omega^2 = \frac{A(T_C - T)}{D} + \rho\omega^2 + \mathrm{i}\omega\Gamma \tag{8}$$

$$\delta_\omega^{-1} = \delta^{-1} - (\rho_S \omega^2 + \mathrm{i}\omega\Gamma_S). \tag{9}$$

The eigenfunctions are solutions of equation (6):

$$\delta P_\omega = C\frac{\sin k_\omega r}{r} \tag{10}$$

and substituting the last expression into equation (7), one obtains the equation for the eigenvalues ω:

$$k_\omega R + \left(\frac{R}{\delta_\omega} - 1 \right) \tan k_\omega R = 0. \tag{11}$$

The system becomes unstable when the frequency of the soft mode is zero. The transition temperature T_P is a solution of equation (11) for $\omega = 0$. To obtain this solution, one should realize that if $T < T_C$, then $k_0^2 \equiv k_{\omega=0}^2 > 0$ (see equation (8)), and equations (10), (11) contain real k_0 for $\omega = 0$. If $T > T_C$ then $k_0^2 < 0$, k_0 is purely imaginary, and equations (10) and (11) can be rewritten as

$$\delta P_{\omega=0} = C\frac{\sinh |k_0| r}{r} \tag{12}$$

$$|k_0| R + \left(\frac{R}{\delta} - 1 \right) \tanh |k_0| R = 0. \tag{13}$$

The graphical representation of equation (11) (and equation (13)) is shown in figure 1. There are also approximative solutions in some cases:

$$T_P = T_C - \frac{3D/A}{R^2}\frac{R}{\delta} \qquad \frac{R}{|\delta|} \ll \frac{1}{4} \qquad (\delta > 0 \text{ or } \delta < 0) \tag{14}$$

$$T_P = \left(T_C - \frac{\pi^2 D/A}{R^2}\right) + \frac{2\pi^2 D/A}{R^2}\left(\frac{\delta}{R}\right)^2 \qquad \frac{R}{\delta} \gg 1 \qquad (\delta > 0) \tag{15}$$

$$T_P = \left(T_C + \frac{D/A}{\delta^2}\right) + \frac{2D/A}{\delta^2}\left(\frac{-\delta}{R}\right) \qquad \frac{R}{-\delta} \gg 1 \qquad (\delta < 0) \tag{16}$$

$$T_P = \left(T_C - \frac{\pi^2 D/A}{4R^2}\right) + \frac{2D/A}{R^2}\left(1 - \frac{R}{\delta}\right) \qquad \left|1 - \frac{R}{\delta}\right| \ll 1 \qquad (\delta > 0). \tag{17}$$

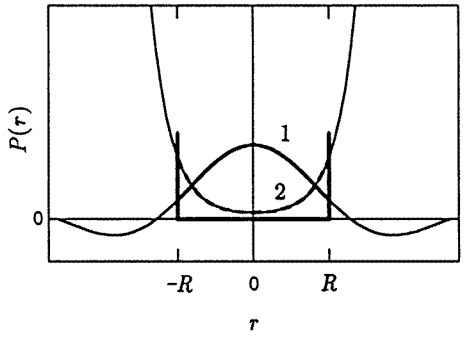

Figure 2. The profile of the soft-mode amplitude: curve 1 is for $T_P < T < T_C$ ($\delta > 0$, equation (10)); and curve 2 is for $T_C < T_P < T$ ($\delta < 0$, equation (12)).

For $\delta > 0$, the Curie temperature $T_P < T_C$, as can be seen also in the limiting-cases equations (14) and (15), and in figure 1. In this case $k_0^2 > 0$, and the spatial distribution of the polarization of the soft mode is described by equation (10); see figure 2. This means that the phase transition occurs over all of the particle volume, and the surface shifts the transition temperature to T_P. For large R, the temperature T_P approaches T_C (see equation (15)), and the surface term in the free energy (2) becomes small compared with the bulk term (i.e., the ratio $R^2\delta^{-1}/R^3 = 1/R\delta \to 0$).

Different behaviour appears for $\delta < 0$. Then $T_P > T_C$, and the shape of the soft mode assumes an exponential character near the surface; see equation (12), and figure 2. The phase transition sets in inside the surface layer, the thickness of which is $k_0^{-1} = \sqrt{A(T_P - T_C)/D}$. This is evident for large radius R (i.e., a planar surface). Then the transition temperature T_P approaches the value $T_C + \delta^{-2}D/A > T_C$, even if the surface term is small ($1/R\delta \to 0$) compared with the particle volume. The polarization becomes nonzero inside the layer near the surface, while it is zero at distances larger than $k_0^{-1} \propto \delta$.

For $\delta > 0$, there can exist a critical radius R_C below which the ferroelectric phase does not exist. The numerical value of R_C is a solution of equation (11), obtained putting $T_P = 0$ and $\omega = 0$. Smaller particles do not undergo the phase transition. The phenomenological formula used in reference [2] has the same form as expression (14). The typical course of the dependence of $t_P \equiv T_P/T_C$ on the radius R is shown in figure 3, where we use the same coefficients as in reference [10].

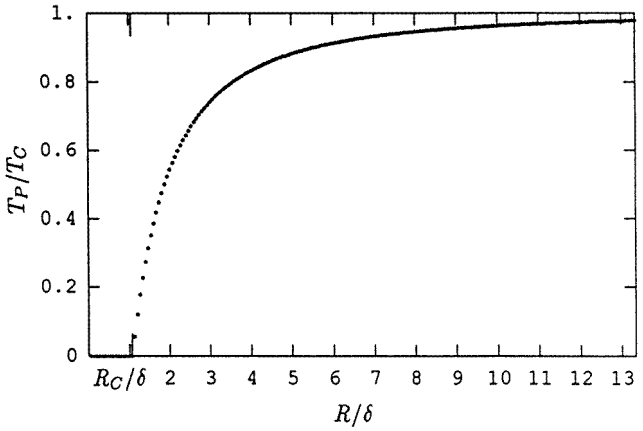

Figure 3. The size dependence of the phase transition temperature $t_P \equiv T_P/T_C$; the parameter used is a dimensionless combination: $\delta\sqrt{AT_C/D} = 15$.

Let us note that if we adopt the size dependence of the parameter δ according to equation (3), then its value becomes always positive for small enough particles.

4. The spatial distribution of the spontaneous polarization

Let us consider a temperature T below the transition temperature T_P. Further, we consider $T_P < T_C$, i.e. $\delta > 0$. The polarization $P(r)$ could be obtained by solving equations (6) and (7), putting $\omega = 0$. Instead of doing this, we assume the profile to have the approximate form

$$P(r) = P_0 \frac{\sin k_p r}{r} \qquad k_p^2 = \frac{A(T_C - T_P)}{D} > 0 \tag{18}$$

where the amplitude P_0 should be calculated. Substituting (18) into (2) and minimizing the free energy, one easily derives the equilibrium value

$$P_0^2 = \frac{-I_1}{I_2}\frac{A}{B}(T_P - T) \qquad T < T_P \tag{19}$$

where

$$I_1 = -4(k_p R)^4\left(1 - \frac{\sin 2k_p R}{2k_p R}\right) \tag{20}$$

$$I_2 = [-3 + 4\cos 2k_p R - \cos 4k_p R + 8k_p R\,\mathrm{Si}(2k_p R) - 4k_p R\,\mathrm{Si}(4k_p R)]k_p. \tag{21}$$

(Si is the sine integral function.)

The average polarization P_{av} over the particle volume is

$$P_{av} = 3P_0\frac{\sin k_p R - k_p R\cos k_p R}{(k_p R)^3}. \tag{22}$$

In a particle with the radius R, the average polarization $P_{av} \propto (T_P - T)^{1/2}$. Let us fix the temperature T, and only vary the radius R. Then $P_{av} \propto (R - R_P)^{1/2}$ for $R > R_P$, and $P_{av} = 0$ for $R < R_P$. R_P is the radius at which the size-driven phase transition occurs. The size dependence of P_{av} according to expression (22) is compared with that calculated numerically; see figure 4. A good agreement occurs near the phase transition driven by

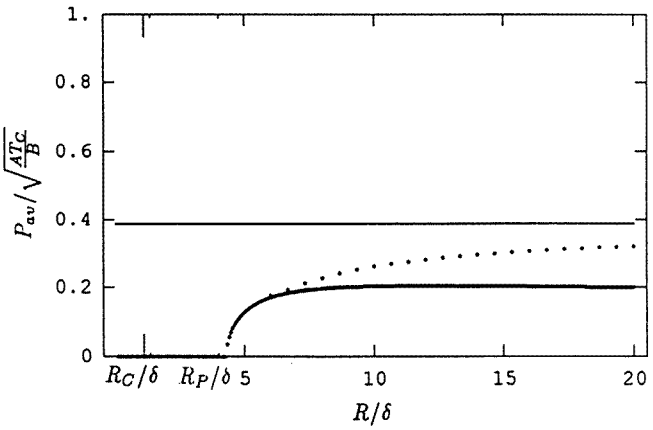

Figure 4. The size dependence of the averaged polarization P_{av} at the temperature $t = 0.85$; the same coefficients were used as for figure 3. Curve 1 (bold curve): expression (22); curve 2 (dotted curve): numerical calculation; and curve 3 (full curve): the bulk value $P_{av}/\sqrt{AT_C/B} = (1-t)^{1/2} \doteq 0.39$.

the change of the particle size ($R_P < R < 7\delta$), while far enough away (for $R > 7\delta$) the polarization departs from the approximative formula (22), approaching the bulk value

$$P_{av} = \frac{A}{B}(T_C - T)^{1/2}$$

for the large particles. This reflects the fact that the *ansatz* (18) is valid for temperatures satisfying the inequalities $(T_P - T)/T_P \ll 1$ and $T_P - T \ll T_C - T_P$. Outside this region, the coefficient of the linear function (19) becomes temperature dependent.

5. Susceptibility

In accord with equations (6) and (7), the equations of motion for dynamic susceptibility read

$$\frac{1}{r}\frac{\partial^2(r\chi_\omega)}{\partial r^2} - \left(-k_\omega^2 + 3\frac{B}{D}P(r)^2\right)\chi_\omega = -\frac{1}{D} \tag{23}$$

$$\frac{\partial \chi_\omega^S}{\partial r} + \left(\frac{1}{\delta_\omega}\right)\chi_\omega^S = 0. \tag{24}$$

First, we study the paraelectric phase, in which $P(r) = 0$. Then the solution of equation (23), finite at $r = 0$, is

$$\chi_\omega(r) = C_\omega \frac{\sin k_\omega r}{r} - \frac{1}{Dk_\omega^2} \tag{25}$$

where the constant C_ω is determined by putting (25) into (24):

$$C_\omega = \frac{R^2}{D}\frac{1}{\left[kR + (R\delta_\omega^{-1} - 1)\tan k_\omega R\right]k_\omega^2\delta_\omega \cos k_\omega R}. \tag{26}$$

Finally, the total susceptibility, derived by integration of $\chi_\omega(r)$ over the volume of the particle, becomes

$$\chi_\omega^{tot} = \frac{4\pi}{V}\int_0^R \mathrm{d}r\ r^2\chi_\omega(r) = \frac{1}{Dk_\omega^2}\left[\frac{\tan k_\omega R - k_\omega R}{(R\delta_\omega^{-1} - 1)\tan k_\omega R + k_\omega R}\frac{3}{\delta_\omega k_\omega^2 R} - 1\right]. \tag{27}$$

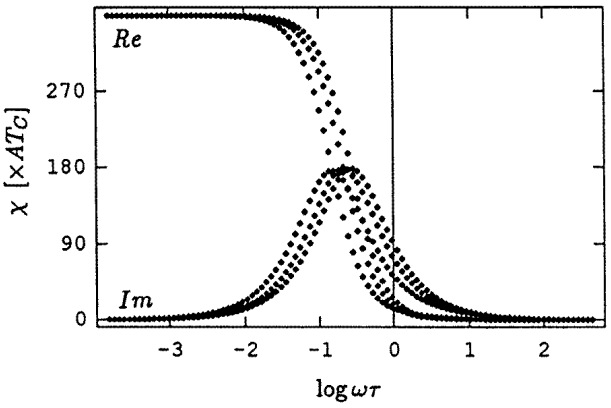

(a)

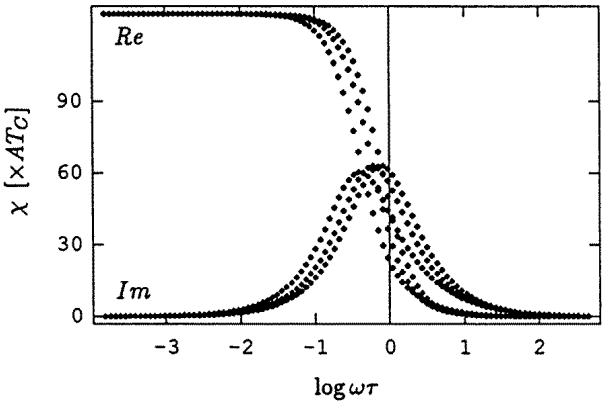

(b)

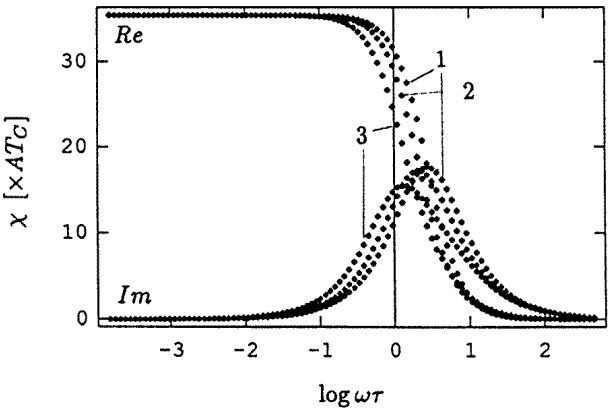

(c)

Figure 5. The dynamic susceptibility of the high-temperature phase; $R/\delta = 4/3$, $\delta\sqrt{AT_C/D} = 15$; (a) $t = 0.5$; (b) $t = 1$; and (c) $t = 3$. The ratio of relaxation times is: $\tau_S/\tau = 0$ (curves 1); $\tau_S/\tau = 0.45$ (curves 2); and $\tau_S/\tau = 1.35$ (curves 3).

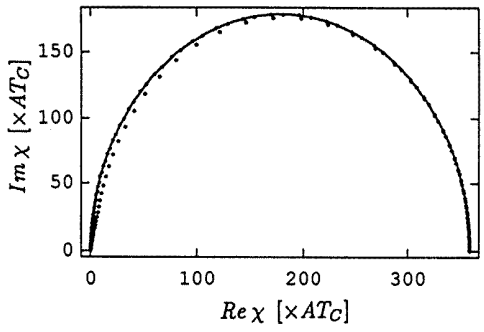

(a)

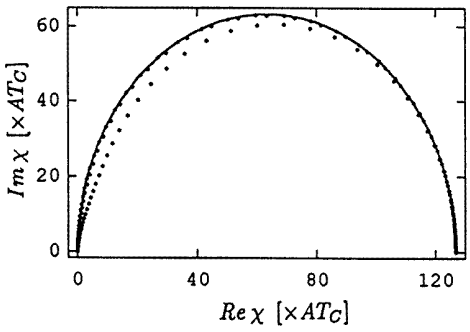

(b)

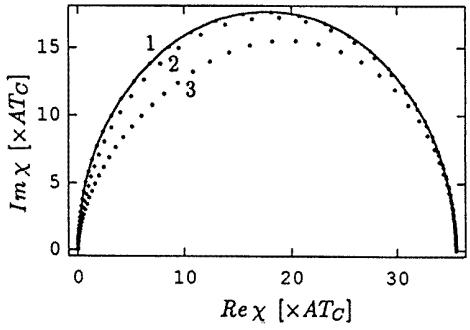

(c)

Figure 6. Cole–Cole plots of the susceptibilities shown in figure 5. (a) $t = 0.5$; (b) $t = 1$; and (c) $t = 3$; $\tau_S/\tau = 0$ (curves 1); $\tau_S/\tau = 0.45$ (curves 2); and $\tau_S/\tau = 1.35$ (curves 3). The full-line semicircle represents the Debye relaxation.

Let us further consider $\rho = \rho_S = 0$. Then one obtains Debye-like relaxation for the bulk crystal:

$$\chi_\omega^{bulk} = \frac{1}{AT_C}\left(\left(\frac{T}{T_C} - 1\right) - \mathrm{i}\omega\tau\right)^{-1}$$

with the high-temperature relaxation time $\tau = \Gamma D/AT_C$. From equation (9), one can also define the characteristic relaxation time of the surface, $\tau_S = \Gamma_S\delta$. Expression (27)

has in general an infinite number of complex zeros, and the spectrum should be more complicated than that for the simple Debye relaxator. The main features are demonstrated in figures 5 and 6. When the ratio τ_S/τ is small, the susceptibility χ_ω^{tot} is well approximated by the Debye relaxator for a wide range of low and high temperatures. The broadening of the high-frequency side of the relaxation peak increases with increasing τ_S/τ and with increasing temperature. In the Cole–Cole diagram, a deviation from the Debye process occurs, and it resembles the more complicated relaxation described by the Havriliak–Negami expression [11].

Let us study the temperature dependence of the susceptibility. We can rewrite k_ω as

$$k_\omega^2 = k_{p,\omega}^2 - \frac{A}{D}(T - T_P) \qquad k_{p,\omega}^2 = \frac{A}{D}(T_C - T_P) + \rho\omega^2 + \mathrm{i}\omega\Gamma \tag{28}$$

and expand χ_ω^{tot} in $T - T_P$:

$$\chi_\omega^{tot} \doteq \frac{1}{Dk_{p,\omega}^2}\left(\left[(\tan k_{p,\omega}R - k_{p,\omega}R)\Big/\left\{[(R\delta_\omega^{-1} - 1)\tan k_{p,\omega}R + k_{p,\omega}R] + \frac{k_{p,\omega}R\tan k_{p,\omega}R + R\delta_\omega}{2k_{p,\omega}R}\frac{AR^2}{D}(T - T_P)\right\}\right]\frac{3}{\delta_\omega k_{p,\omega}^2 R} - 1\right). \tag{29}$$

For nonzero ω, the dynamic susceptibility does not diverge at T_P. The static susceptibility χ_0^{tot} exhibits Curie–Weiss behaviour near T_P:

$$\chi_0^{tot} \doteq \frac{1}{Dk_p^2}\left(\frac{\tan k_pR - k_pR}{k_pR\tan k_pR + R\delta^{-1}}\frac{6D}{A\delta k_pR^2}\frac{1}{T - T_P}\right) \tag{30}$$

where $T > T_P$ and $k_p \equiv k_{p,0}$. The Curie constant and T_P are functions of the radius R.

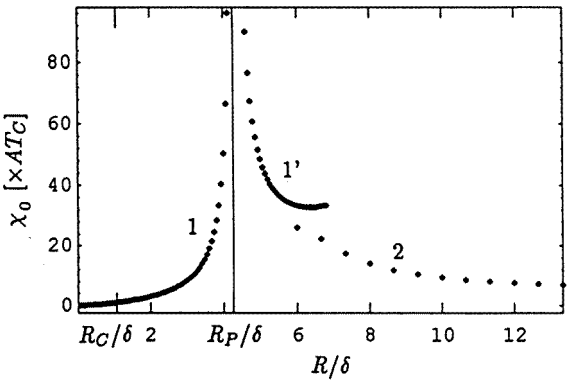

Figure 7. The size dependence of the static susceptibility χ_0 at the temperature $t = T/T_C = 0.85$; $\delta\sqrt{AT_C/D} = 15$. R_C is the critical radius, and R_P is the radius for which $t_P = t$. Curves 1 and 1′ are obtained from formula (27) (see the text); and curve 2 shows the numerical results.

Expanding expression (27) in $R_P - R$, one can obtain the size dependence of the susceptibility at the fixed temperature T. The radius R_P is the one for which the transition temperature $T_P = T$. The static susceptibility reads

$$\chi_0^{tot} \doteq \frac{1}{Dk_0^2}\left(\frac{\tan k_0R_P - k_0R_P}{(k_0^2R_P - \delta^{-1})\tan k_0R_P - R_P\delta^{-1}k_0}\frac{3}{\delta k_0^2R_P}\frac{1}{R_P - R}\right) \tag{31}$$

where $R < R_P$ and the particle is in the paraelectric state. To study the susceptibility of the ferroelectric phase, i.e. where $R > R_P$ or $T < T_P$, one should solve equation (23) using the

polarization profile $P(r)$ given by equation (18). This is a difficult task, and for simplicity we put $P(r) = P_{av}$ in equation (23); P_{av} is determined by equation (22), and depends on R and T. Then the susceptibility again has the form of equation (27) (and of equations (30) and (31)), but with the renormalized wave-vector

$$k_\omega^2 = \frac{A(T_C - T)}{D} - 3\frac{B}{D}P_{av}^2 + \mathrm{i}\omega\Gamma$$

and with $T < T_P$ and $R > R_P$. So the susceptibility obeys the Curie–Weiss law from both sides of the phase transition, i.e. $\chi_0^{tot} \propto 1/|R - R_P|$ and $\chi_0^{tot} \propto 1/|T - T_P|$. The size dependence of the static susceptibility is plotted in figure 7. The approximative solution considered above is valid just above R_P, as follows from the comparison with the exact (numerical) solution. Note that the susceptibility exhibits a peak (it diverges due to the second-order phase transition) at $R = R_P$. A similar maximum of the size-dependent dielectric constant was observed for $BaTiO_3$ [8], and explained alternatively in reference [9].

6. Conclusions

We have analytically investigated the Landau-type model of the second-order ferroelectric phase transition in small particles that was recently studied numerically, as described in reference [10]. The model assumes that the surface charges are fully compensated, and that the phase transition is modified mainly due to the different properties of the surface layer.

Our main results concern both static and dynamic properties. The size dependence of the transition temperature could change from $T_C - T_P \propto 1/R$ to $T_C - T_P \propto 1/R^2$ on varying the coefficients and the radius; see equations (14)–(17). The former case has been used in the literature [2]. Below T_P, the order parameter is position dependent, with a Landau-type temperature behaviour. The approximative profile (18) is valid near the phase transition point; see figure 3.

The dynamic dielectric susceptibility is more complicated than a simple Debye-like relaxation. This difference increases with the ratio of surface and bulk relaxation times τ_S/τ, and with increasing temperature. The asymmetric Cole–Cole plot resembles the Havriliak–Negami stretched relaxation. Note that the assumption of full compensation can be justified for the low-frequency region. However, at higher frequencies, the compensating charges are retarded with respect to the oscillating polarization, and the depolarization field that arises causes further broadening of the high-frequency part of the dielectric dispersion.

The static susceptibility obeys a typical Curie–Weiss temperature dependence. The size dependence exhibits similar behaviour: at a given temperature T, the divergence occurs for particles with the radius $R_P(T)$; see figure 7. This is in accord with the maximum of static susceptibility observed for $BaTiO_3$ [8]. Particles with radii smaller than R_P are in the paraelectric state, while those with radii larger than R_P are in the ferroelectric state.

Note that the size-driven phase transition, and the similar behaviour of the polarization and susceptibility discussed in this paper can be obtained also within a model in which just the depolarization field is considered [9]. Therefore it is sometimes rather difficult to choose the more appropriate model; e.g., both approaches have been used in the discussion of experiments on ceramics and powders of $BaTiO_3$ [9, 12].

In composite materials, the irregular shapes of the particles (causing δ to become a function of the position), as well as a distribution of particle sizes, the randomness of the particle surroundings, and interparticle interactions, lead to a more complex picture of the phase transition [13].

Acknowledgments

The authors would like to sincerely thank J Petzelt for fruitful discussions and comments. This work was supported by the Grant Agency of the Czech Republic, Projects No 202/96/0425 and No 202/95/1393.

References

[1] Uchino K, Sadanaga E and Hirose T 1989 *J. Am. Ceram. Soc.* **72** 1555
[2] Ishikawa K, Yoshikawa K and Okada N 1988 *Phys. Rev.* B **37** 5852
[3] Jona F and Shirane G 1962 *Ferroelectric Crystals* (New York: Dover)
[4] Scott J F, Duiker H M, Beale P D, Pouligny B, Dimmler K, Parris M, Butler D and Eaton S 1988 *Physica* B **150** 160
[5] Hadni A and Thomas R 1984 *Ferroelectrics* **59** 221
[6] Batra I P and Silverman B D 1972 *Solid State Commun.* **11** 291
[7] Lee M-H, Halliyal A and Newnham R E 1988 *Ferroelectrics* **87** 71
[8] Arlt G, Hennings D and de With G 1985 *J. Appl. Phys.* **58** 1619
[9] Shih Wan Y, Shih Wei-Heng and Aksay I A 1994 *Phys. Rev.* B **50** 15 575
[10] Zhong W L, Wang Y G, Zhang P L and Qu B D 1994 *Phys. Rev.* B **50** 698
[11] Jonscher A K 1983 *Dielectric Relaxation in Solids* (London: Chelsea Dielectrics)
[12] Schlag S, Eicke H-F and Stern W B 1995 *Ferroelectrics* **173** 351
[13] Hudák O, unpublished